HHS Public Access

Author manuscript

Neuron. Author manuscript; available in PMC 2015 June 24.

Published in final edited form as:

Neuron. 2014 December 17; 84(6): 1273–1286. doi:10.1016/j.neuron.2014.11.016.

Fmr1 KO and Fenobam Treatment Differentially Impact Distinct Synapse Populations of Mouse Neocortex

Gordon X. Wang[1,2,*], **Stephen J Smith**[2,4], and **Philippe Mourrain**[1,3]

[1]Center for Sleep Sciences and Medicine, Department of Psychiatry and Behavioral Sciences, Stanford University, Stanford, CA 94305, USA

[2]Department of Molecular and Cellular Physiology, Stanford University, Stanford, CA 94305, USA

[3]INSERM 1024, Ecole Normale Supérieure Paris, 75005, France

[4]Allen Institute for Brain Science, Seattle, WA 98103, USA

SUMMARY

Cognitive deficits in fragile X syndrome (FXS) are attributed to molecular abnormalities of the brain's vast and heterogeneous synapse populations. Unfortunately, the density of synapses coupled with their molecular heterogeneity presents formidable challenges in understanding the specific contribution of synapse changes in FXS. We demonstrate powerful new methods for the large-scale molecular analysis of individual synapses that allow quantification of numerous specific changes in synapse populations present in the cortex of a mouse model of FXS. Analysis of nearly a million individual synapses reveals distinct, quantitative changes in synaptic proteins distributed across over 6,000 pairwise metrics. Some, but not all, of these synaptic alterations are reversed by treatment with the candidate therapeutic fenobam, an mGluR5 antagonist. These patterns of widespread, but diverse synaptic protein changes in response to global perturbation suggest that FXS and its treatment must be understood as a networked system at the synapse level.

INTRODUCTION

Cognitive deficits in neurological diseases are often attributed to synapse abnormalities (Bhakar et al., 2012; Coghlan et al., 2012; Garden and La Spada, 2012; Grant, 2012; Sheng et al., 2012). The understanding of these abnormalities is complicated by the heterogeneity of the brain's vast synapse populations (Bayés et al., 2011; Emes and Grant, 2012; O'Rourke et al., 2012). Unfortunately, the methods used to quantify synaptic abnormalities in these diseases are either too narrow (direct recording from single cells) or too broad (homogenized tissue from entire brain regions) to capture the expected range and detail of synaptic deficits. For example, previous studies have used assays of total cellular protein

*Correspondence: drwonder@gmail.com.

SUPPLEMENTAL INFORMATION

Supplemental Information includes seven figures, one table, and Supplemental Experimental Procedures and can be found with this article online at http://dx.doi.org/10.1016/j.neuron.2014.11.016.

AUTHOR CONTRIBUTIONS

G.X.W. designed, performed, and analyzed all experiments. G.X.W. wrote all software used for the analysis of the data. G.X.W., S.J.S., and P.M. wrote the paper.

expression as surrogates of synaptic protein changes in diseased brains, but it is highly likely that synaptic and total cellular protein levels are independently regulated. Methods that can capture the expected scope of neurological deficits with single-synapse resolution are thus needed. Such methods should facilitate the detailed understanding of disease-wrought changes in the synapse population (Defelipe, 2011; O'Rourke et al., 2012) and provide better pharmaceutical targets in normalizing the perturbed ecology of the synaptic landscape (Cummings et al., 2013; Henderson et al., 2013).

FXS is a genetic disorder associated with intellectual disability and is the leading monogenic cause of autism. It is caused by the epigenetic silencing of a single gene, fragile×mental retardation 1 (*Fmr1*) (Pieretti et al., 1991; Verkerk et al., 1991). The singular loss of the *Fmr1* gene product, fragile X mental retardation protein (FMRP), leads to the perturbation of a number of highly interconnected molecular signaling cascades that underlie a large number of important neuronal and synaptic processes (Grewal et al., 1999; Hoeffer and Klann, 2010; Shiflett and Balleine, 2011; Sweatt, 2001; Thiels and Klann, 2001). For example, mammalian target of rapamycin (mTOR) and extracellular signal-related kinase (ERK) are implicated in FXS synapse dysfunction (Bhakar et al., 2012; Gallagher et al., 2004; Osterweil et al., 2013; Sharma et al., 2010), and they are both well-known signal transduction hubs that are involved in regulating a number of neuronal processes including synaptic plasticity, dendritic development, and local translation. (Grewal et al., 1999; Hoeffer and Klann, 2010; Kindler and Kreienkamp, 2012; Sweatt, 2001; Thiels and Klann, 2001). Thus, one would expect a wide range of synaptic perturbations in FXS that have not been quantified to date.

The association of abnormal dendritic spine morphology and density with FMRP loss has been a major focus of FXS research (Comery et al., 1997; Cruz-Martín et al., 2010; Galvez and Greenough, 2005; Galvez et al., 2003; Lauterborn et al., 2013; Nimchinsky et al., 2001). Spines are important in that they represent structural proxies of cortical excitatory synapses (Tada and Sheng, 2006; Nimchinsky et al., 2002; Segal, 2005; Yuste and Bonhoeffer, 2001). However, to date, few studies have directly quantified excitatory synapse changes in FXS. Moreover, previous studies of dendritic spine density have revealed heterogeneous responses to FMRP loss that are age, cell type, and brain area specific (Cruz-Martín et al., 2012; Galvez and Greenough, 2005; Lauterborn et al., 2013; Nimchinsky et al., 2001; Till et al., 2012; Wijetunge et al., 2014). It is clear, however, that glutamatergic mechanisms that modulate excitatory synapse formation and elimination are affected by FMRP loss (Auerbach et al., 2011; Le Duigou et al., 2011; Gallagher et al., 2004; Huber et al., 2000; Vinueza Veloz et al., 2012; Zhang and Alger, 2010). Yet, the full extent and implication of those mechanistic changes on the synapse population has not been described. Inhibitory synapses are also affected by FMRP loss, but how their density or molecular characteristics are changed remains mostly undefined (Adusei et al., 2010; D'Hulst et al., 2009; Gibson et al., 2008; El Idrissi et al., 2005). The present study is designed to quantify density and molecular changes, due to FMRP loss, in both excitatory and inhibitory synapses, with a detailed focus on excitatory synapse populations.

Progress in defining the molecular dysfunction in *Fmr1* knockout (KO) synapses has made FXS one of a few neurodevelopmental diseases with targeted drugs in clinical trials (Berry-

Kravis et al., 2012; Dölen et al., 2010; Michalon et al., 2012). Metabotropic glutamate receptor 5 (mGluR5) is a major pharmaceutical target for the treatment of FXS in humans (Bhakar et al., 2012; Dölen et al., 2010; Robertson, 2013). Antagonists against mGluR5, including the highly selective compound fenobam (Berry-Kravis et al., 2009; Vinueza Veloz et al., 2012; de Vrij et al., 2008), are effective in alleviating some behavioral and neuronal perturbations caused by FMRP loss in mice (Auerbach et al., 2011; Dölen and Bear, 2008; Michalon et al., 2012; Wijetunge et al., 2008). However, antagonism of mGluR5 leads to heterogeneous changes in the expression of long-term depression, long-term potentiation, and homeostatic plasticity in a region- and layer-specific manner in the cortex (Anwyl, 2009; Hu et al., 2010; Tsanov and Manahan-Vaughan, 2009; Ueta et al., 2008). Such complexity of mGluR5 antagonism greatly complicates mechanistic interpretation of mGluR5 function in FXS and suggests a diversity of pharmacological efficacy that has not yet been experimentally verified.

Thus, to better quantify the synaptic etiology of FXS and bring new understanding to its treatment, systematic analysis of the effects of FMRP loss on the heterogeneous circuit and synaptic elements of the brain is needed. To this end, we combined the subdiffraction, molecular imaging capabilities of array tomography (AT) (Micheva and Smith, 2007; Wang and Smith, 2012) with a computational synapse classification algorithm. This algorithm allows for the analysis of molecularly defined synapse classes that belong to specific functional circuits. This analysis generated over 6,000 synapse metrics incorporating over 1 million excitatory and inhibitory synapses of cortical-cortical and thalamocortical neural circuits distributed across layers 4 and 5 of the mouse somatosensory cortex. The single-synapse-level resolution combined with the numeric and spatial coverage of the data set allowed us an unprecedented system-level view of the fine scale, quantitative changes in the synapse population that are mediated by systemic loss of FMRP and its pharmacological rescue by fenobam.

We found that the loss of this single gene product causes a formidable transformation of the synaptic landscape in the KO cortex. *Fmr1* loss generates distinct synaptic phenotypes across the entire synapse population. The expression of these phenotypes depends on the circuit and the cortical layer. For instance, the density of total excitatory synapses is elevated in layer 4, while it is unchanged in layer 5. However, in layer 5, synapses of the thalamocortical circuit are specifically decreased. Moreover, the response of these synaptic phenotypes to fenobam treatment is also specific to the molecular composition and cortical layer of the synapses studied, and while this study demonstrates that fenobam treatment can be highly effective in rescuing many synaptic perturbations, its efficacy can be limited to specific synaptic subsets. For example, the molecular composition of layer 4 thalamocortical synapses is not effectively rescued by fenobam treatment, while layer 5 thalamocortical synapses are. Thus, the data in this work illustrate that the diversity of neural circuits, cell types, and synapse classes react distinctly to global perturbations, even if those perturbations are initiated by a single ubiquitous gene or drug. The results of this study demonstrate the complex problems that challenge our understanding of neurological diseases and their treatments, but this study also provides new methodology to solve these problems and demonstrates how data can be acquired to constrain and describe disease-mediated synaptic

changes at a systems level. Thus, this study provides a unique profile of system-level synaptic deficits in FXS and presents methods of molecularly constrained synapse analysis that can generate quantitative metrics for the evaluation of synapse population changes and their rescue by therapeutics.

RESULTS

AT Enables Robust Computational Classification of Cortical Synapses

AT provides spatially multiplexed protein data that allow for the identification of synapses through the correlated localization of synaptic molecules (Figure 1; Figure S1 available online). For example, glutamatergic synapses can be found by the apposition of postsynaptic density 95 (PSD95), synapsin-1 (SYN), and a vesicular glutamate transporter (VGluT) (Figure 1B, white arrowheads). GABAergic synapses can be found by the apposition of gephyrin (GPHN), vesicular GABA transporter (VGAT), and glutamate decarboxylase (GAD) (Figure 1B, yellow arrowheads). Each of our data sets contains hundreds of thousands of such protein localizations (Figures 1 and S1). Computational methods are therefore necessary to quantify the synaptic information contained in these data sets.

We used the local orientation and distance of synaptic protein puncta in conjunction with consensus structural characteristics of a cortical synapse (De Camilli et al., 1983; Chen et al., 2008; Heuser and Reese, 1977; Hunt et al., 1996) to classify synapses based on their molecular orientation and composition. Specifically, punctum objects are segmented using a thresholded connected-components analysis. Then, excitatory synapse classification is initiated by computing a local-synapse vector between the centers of mass of a postsynaptic PSD95 punctum and a presynaptic SYN punctum (Figure 1C; also see Experimental Procedures for addition details). The magnitude of that synaptic vector, which is the distance (*d1* in Figure 1C) between PSD95 and SYN centers, is used to define a unique colocalization sphere for each candidate synapse. Any protein centers from other protein channels that fall within this sphere are considered colocalized to the candidate synapse. The verification of candidate excitatory synapses uses a third protein channel of known synaptic localization, such as vesicular glutamate transporter 1 (VGluT1), so that the representative ratification of a VGluT1 synapse requires a presynaptic VGluT1 center to be closer to SYN than PSD95 (Figure 1C). This logic also holds for inhibitory synapses with postsynaptic GPHN, presynaptic VGAT, and GAD as the third presynaptic inhibitory marker. This method generates molecularly defined synapse classes that are robust against variations in image segmentation thresholds (Figures S2A–S2I) and consistent with human classified data (Figure S2J) (Micheva et al., 2010).

Using analogous methods with additional proteins, 25 molecularly defined synapse classes were generated (Figure 2A) in 34 mice across four conditions (wild-type [WT], *Fmr1* KO, fenobam-treated WT, and fenobam-treated *Fmr1* KO). These 25 synapse classes form a distinct hierarchy that represent specific molecular combinations of proteins in the data set that were determined a priori to be of interest in FXS etiology. Excitatory and inhibitory synapse types form the basis of all 25 classes. Excitatory synapses are further divided by whether they contain VGluT1, VGluT2, or both proteins. These excitatory classes represent genetically defined synaptic types that do not transit between each other (Figure S3)

(Fremeau et al., 2001; Graziano et al., 2008; Herzog et al., 2001; Kaneko and Fujiyama, 2002; Nahmani and Erisir, 2005; Nakamura et al., 2005). These genetically defined excitatory synapse classes are further subdivided by the combination of other molecular markers in those synapses, such as synaptopodin (SYNPO) and Fragile X-related proteins 1 and 2 (FXR1P and FXR2P). These molecularly defined subclasses represent more plastic synapse types. For example, SYNPO synapses represent mature dendritic spines whose identity can be modified by learning or other environmental factors (Deller et al., 2000, 2003; Holbro et al., 2009; Segal et al., 2010; Vlachos et al., 2009).

We used these methods to analyze layers 4 and 5 of the adult (4-months-old) mouse somatosensory cortex (Figure 2B). These two cortical layers were selected because sensory information processing is a known behavioral deficit in FXS patients and *Fmr1* KO mice (Baranek et al., 2008; Hoeft et al., 2010; Kogan et al., 2004; Ventura et al., 2004; Yan et al., 2004). Layers 4 and 5 represent, respectively, the majority of direct thalamic-sensory input and the integrated cortical network output of the cortex (Aronoff et al., 2010; Douglas and Martin, 2004; Feldmeyer and Sakmann, 2000; Lübke and Feldmeyer, 2007; Schubert et al., 2007). In total, over a million synapses were analyzed across four animal conditions generating over 6,000 potential pairwise metrics.

Effects of Fmr1 KO and Fenobam Treatment Are Layer and Circuit Specific

A layer- and circuit-specific analysis of cortical volumetric synapse density changes in response to FMRP loss is currently unavailable. Therefore, we directly compared the average ratios of *Fmr1* KO and WT excitatory synapse density from layers 4 and 5 of the mouse somatosensory cortex (Figure 3). Ratios are used because tissue from KO and WT brains were paired starting at fixation to reduce variability caused by tissue processing, immunohistochemistry, and imaging (see Experimental Procedures). In layer 4 the density of total excitatory synapses is significantly elevated in KO mice, even after adjustment for multiple comparisons using Benjamini-Hochberg false discovery rate calculations ($q < 0.05$; see Experimental Procedures). In contrast, the total excitatory synapse density in layer 5 is not significantly different between KO and WT ($q > 0.05$; Figure 3A).

To study the changes in excitatory synapse density in more detail, we subclassified excitatory synapses by their VGluT composition. The two major cortical VGluTs (VGluT1 and VGluT2) are ideal for the discrimination of excitatory synapses because they represent markers of specific cortical circuits, such that VGluT1 is expressed in the majority of cortical-cortical synapses and VGluT2 is expressed in the majority thalamocortical synapses. (Fremeau et al., 2001; Graziano et al., 2008; Herzog et al., 2001; Kaneko and Fujiyama, 2002; Nahmani and Erisir, 2005; Nakamura et al., 2005). This class-specific analysis uncovers specific variation in of *Fmr1* KO synapse densities (Figures 3B and 3C) such that the density of layer 5 VGluT2 synapses, unlike layer 5 total excitatory synapse density, is significantly decreased, while all excitatory synapse classes are elevated in layer 4, in agreement with layer 4 total synapse density increase ($q < 0.05$; Figures 3B and 3C). This demonstrates that FMRP loss differentially affects synapses in thalamocortical (VGluT2) and cortico-cortical (VGluT1) circuits in a manner that is layer and class specific.

To explore the extent to which fenobam treatment reverses these circuit- and layer-specific effects of *Fmr1* KO, we orally administered fenobam (100 mg per kg body weight) to *Fmr1* KO mice for 2 weeks (see Experimental Procedures for more details). Comparison of these animals with paired WT animals (Figures 3D–3F) revealed that, with the exception of layer 4 VGluT1/2 synapses, fenobam treatment rescued density changes across all other synapse classes in both cortical layers of the KO (Figures 3E and 3F). Layer 4 VGluT1/2 synapse density, which was significantly elevated in the KO, was reduced by fenobam, but this reduction led to a significant density decrease of this synapse class ($q < 0.05$; Figures 3E and 3F). Furthermore, control tests of fenobam in WT animals showed that by itself fenobam did not significantly modify synapse density in these synapse classes, demonstrating that the fenobam effects are specific to the KO (Figures 3G–3I). This shows that fenobam can be highly effective in treating many synapse density deficits mediated by FMRP loss. However, drug treatment may produce its own specific synaptic changes as in layer 4 VGluT1/2 synapse class.

Cellular and Synaptic Protein Levels Are Not Always Correlated

We next assessed whether synaptic protein content reflects total cellular protein expression. To accomplish this, we compared the density and integrated intensity of total and synaptic protein puncta. Together, the density and integrated intensity metrics represent a quantitative measure of the relative protein content present in the tissue volume. In layer 4, neither the density nor the integrated intensity of total VGluT2 puncta are significantly changed between KO and WT ($q > 0.05$; Figures S3B and S4I). Nonetheless, the density of layer 4 VGluT2-containing synapses is significantly increased in the KO ($q < 0.05$; Figure 3C). Thus, the layer 4 VGluT2 synapse density increase mediated by FMRP loss is not due to a total cellular increase in VGluT2 protein level. This reveals that synapse density is not necessarily connected to total protein levels. Moreover, total and synaptic protein level changes can also be disconnected. For example, total VGluT1 protein density and integrated intensity is unchanged in the KO (Figures S3B and S4I), while KO VGluT1 synapse density and integrated intensity is increased (Figures 3C and S4I), revealing a specific increase in synaptic VGluT1 protein but not in total cellular VGLuT1 protein levels.

In layer 5 results are again different. In the KO, the total VGluT2 punctum density is decreased ($q < 0.05$, Figure S3A), without a change in integrated intensity (Figure S4A), matching the significant reduction in the density of KO VGluT2-containing synapses (Figure 3B). This represents a case in which synapse and total protein levels are in agreement. Layer 5 VGluT1 synapse density is also unchanged (Figure 3B) in agreement with layer 5 VGluT1 total protein punctum density in *Fmr1* KO (Figure S3A), but the integrated intensity of layer 5 synaptic VGluT1 puncta is increased in the KO, unlike the total VGluT1 punctum integrated intensity, which is not significantly different from WT (Figure S4A). This demonstrates that FMRP loss specifically increases the VGluT1 protein content of synapses without affecting the number of VGluT1 synapses and the protein content of cellular VGluT1 puncta, in layer 5. Thus, our data reveal an imperfect correlation between total cellular protein levels and synaptic protein levels and demonstrate the need for synapse-specific analysis, as compared to tissue-specific analysis, to resolve synaptic protein differences mediated by cellular perturbations.

FMRP Loss Induces Fenobam-Reversible Decrease in SYNPO-Containing Mature Dendritic Spines

SYNPO is a key regulator of mGluR-mediated spine plasticity and a marker of mature dendritic spines (Deller et al., 2000, 2003; Holbro et al., 2009; Segal et al., 2010; Vlachos et al., 2009). This establishes SYNPO as protein of substantial interest for FXS-mediated synaptic phenotypes (Comery et al., 1997; Dölen and Bear, 2008; Galvez et al., 2003; Vinueza Veloz et al., 2012; Zhang et al., 2009). In *Fmr1* KO animals, there is an overall decrease in total SYNPO punctum density in both layers (Figure S3), while their integrated punctum intensity is not changed (Figures S4A and S4I). This reveals a general decrease in the expression of SYNPO protein in the KO. Yet, the total SYNPO-containing synapse density is unaffected in both layers ($q > 0.05$, Figure 4A), suggesting that the overall density of SYNPO-containing spines is stable in spite of the decrease in total protein levels.

Significant effects of FMRP loss, however, are unmasked by the breakdown of synapse classes. In layer 5, SYNPO-containing VGluT2 synapses are significantly reduced in the KO ($q < 0.05$; Figure 4B), consistent with the overall loss of layer 5 VGluT2 synapses in the KO ($q < 0.05$; Figures 3B and S3A). In layer 4 of KO mice, SYNPO-containing VGluT1 synapse density is depressed compared to WT ($q < 0.05$; Figure 4B) even though the total layer 4 VGluT1 synapse density is increased (Figure 3C). This reveals a selective decrease in SYNPO-containing layer 4 VGluT1 synapses in response to FMRP loss, suggesting that there is a specific decrease in layer 4 mature SYNPO-containing dendritic spines that receive cortical input.

Thus, the global loss of FMRP mediates alterations of SYNPO synapse density that is highly population specific and layer specific. The oral application of fenobam is effective in rescuing the loss of total SYNPO punctum ($q < 0.05$; Figure S3) and class-specific SYNPO synapse density changes in KO animals across both layers ($q > 0.05$; Figures 4C and 4D). This suggests that mGluR5 signaling is an important regulator of the cellular and synaptic expression of SYNPO, which is further reinforced by data generated by the fenobam treatment of WT animals. Analysis of fenobam-treated WT animals reveals that while layer 4 total SYNPO synapse density is not increased, layer 5 total SYNPO synapse density is significantly elevated ($q < 0.05$; Figure 4E), and this increase is primarily due to a significant increase in layer 5 SYNPO VGluT1 synapses ($q < 0.05$; Figure 4F). This concurs with the data suggesting that SYNPO is an important regulator of mGluR5-mediated signaling (Deller et al., 2000, 2003; Holbro et al., 2009; Segal et al., 2010; Vlachos et al., 2009) and that perturbation of mGluR5 signaling affects the synaptic localization of SYNPO. Moreover, the fact that the loss of FMRP in layer 5 abolishes this fenobam-mediated increase in SYNPO VGluT1 synapses means that FMRP action is directly involved in this mGluR5 mediated increase.

Fenobam treatment in WT did not increase layer 5 SYNPO VGluT2 synapse density levels (Figure 4F), which suggest that fenobam directly rescues FMRP-loss-mediated SYNPO VGluT2 synapse loss (Figures 4B and 4D). Layer 4 again presents a different scenario: layer 4 SYNPO VGluT1 synapses are also elevated in WT fenobam-treated animals ($q < 0.05$; Figure 4F), even though the total SYNPO synapse density in layer 4 is not affected (Figure

4E). This increase of layer 4 SYNPO VGluT1 synapses in fenobam-treated WT animals suggests that the normalization of layer 4 SYNPO VGluT1 synapse density in the KO (Figure 3F) might not be a direct rescue by fenobam but a potential occlusion of the KO-mediated decrease by the fenobam-induced synapse density increase (Figures 4B and 4D). These data reveal that the specificity and efficacy of drug action is also subject to variation dependent upon synapse class and cortical layer.

Levels of FXR1P and 2P Expression Are Differentially Impacted by FMRP KO and Fenobam Rescue

FXR1P and FXR2P are nearly structurally identical autosomal homologs of FMRP (Adams-Cioaba et al., 2010; Tamanini et al., 1997, 1999). FXRs are known to form heteromeric complexes with FMRP in neurons (Ceman et al., 1999; Christie et al., 2009; Tamanini et al., 1999). Unfortunately, their involvements in FXS and their synaptic function remain largely unknown. We find the response of FXR2P to FMRP loss to be highly layer specific. FXR2P synapse density and total puncta density are both dramatically decreased in layer 5 KO animals ($q < 0.05$; Figures 5A and S3A) but not in layer 4 ($q > 0.05$; Figures 5A and S3), and this reduction is entirely nonresponsive to fenobam rescue ($q < 0.05$, Figure 5B). These data suggest that in layer 5, FXR2P expression is highly dependent on the presence of FMRP and is independent of mGluR5 signaling. In agreement with the density data, layer 5 integrated intensity metrics for layer 5 VGluT1 synapses reveal a decrease in FXR2P protein content in those synapses (Figure S4A). This synaptic decrease of FXR2P protein content, however, is again synapse class dependent, as FXR2P puncta levels are increased in KO VGluT2 synapses (Figure S4A) even though VGluT2 synapse density is dramatically reduced (Figure 5A). This illustrates that in layer 5 fewer VGluT2 synapses contain FXR2P, but when they are found at those synapses, they are there at greater amounts. Also in agreement with the notion that mGluR5 signaling does not affect FXR2P expression, fenobam treatment of WT animals did not affect FXR2 synapse densities in either layers 4 or 5 (Figure 5C).

The density of FXR1P-containing synapses does not respond to FMRP loss in either cortical layer ($q < 0.05$; Figure S5) and is also independent of mGluR5 signaling (Figure S5). FXR1P total and synaptic integrated intensity is also unaffected in *Fmr1* KO (Figure S4). In layer 5, however, the total puncta density of FXR1P is elevated by FMRP loss (Figure S3). This increase can be rescued by fenobam treatment ($q < 0.05$; Figure S3A), which suggests that layer 5 mGluR5 signaling regulates cellular FXR1P protein levels, but not synaptic FXR1P levels.

Fenobam Rescues Fmr1 KO-Mediated Inhibitory Synapse Increases

The analysis of GPHN-containing GABAergic synapses in layers 4 and 5 of the cortex reveals a significant density increase in inhibitory synapses of both layers of the KO ($q < 0.05$; Figure 6A). This density increase maintains the ratio of GABAergic synapse density to the total glutamatergic synapse density, as the percentage of GABAergic synapses to the total synapse number remains the same in both WT and KO (Figure 6B). This suggests that the GABA system may be responding to changes in the glutamatergic system, which is a synapse plasticity phenomenon that is well documented in sensory cortices (Li et al., 2009;

Maffei et al., 2006; Micheva and Beaulieu, 1995). Fenobam treatment provides further support for the role of glutamate signaling in this inhibitory synapse density increase, as it rescues the GABAergic synapse density increase in layer 4, and reduces the density of layer 5 GABAergic synapses to below WT levels (Figure 6A). This fenobam effect is specific to the FMRP-mediated mechanisms, as fenobam treatment in WT animals did not affect GABAergic synapse densities (Figure 6A).

Fmr1 KO Alters the Molecular Composition of Synapse Populations

Our findings indicate that *Fmr1* KO impacts diverse synapse populations differentially across a wide range of measures. Pairwise comparisons, while informative, do not readily provide a quantitative, statistical measure of the integrated changes occurring in the data set. Thus to provide a more integrated approach to evaluate the synapse data, multivariate logistic regressions can be used to reveal system-level trends in our measurements of synaptic protein level (puncta intensity and puncta integrated intensity) and synaptic protein structure (puncta volume and punctum distance from PSD) (Hosmer and Lemeshow, 2000). Logistic regressions can generate functions that quantitatively relate changes in the molecular features of a synapse (the independent variables) to the probability of that synapse being KO or WT (the binomial dependent variable, KO = 1, WT = 0; see Experimental Procedures).

The application of this regression on 57,480 WT and 66,702 KO synapses, pooled from five animals of each genotype, generates a set of probabilities that represents the likelihood of whether a synapse is KO or WT based on the molecular measures associated with each synapse. Thus, the histograms generated from these probabilities visually represent the quantitative, statistical difference between KO and WT as defined by molecular properties of proteins associated with each population of synapses. Assessing these histograms it is clearly evident from the separation of peaks and the significantly different distributions (Kruskal-Wallis $p < 0.01$; Figures 7A, 7B, 7E, and 7F) that both layer 5 and layer 4 KO synapse populations are molecularly different from their WT counterparts (Figure 7). Moreover, regression analysis shows that layer 5 KO and WT synapse populations are more separated from each other than layer 4 synapse populations (Figure 7). However, pairwise synapse density measures demonstrated that layer 4 synapses are more affected by FMRP loss than those in layer 5 (Figure 3). This illustrates that single metrics cannot fully describe the synaptic deficits seen in *Fmr1* KO mice and that synapse-modifying mechanisms engaged by FMRP loss vary across cortical layers. This layer-specific difference carries over to the response of the synapse populations to fenobam. Layer 5 synapse molecular features in *Fmr1* KO animals are fully rescued by fenobam treatment (Kruskal-Wallis $p < 0.01$; Figure 7C), while in layer 4, the change between KO and fenobam-treated KO synapse populations is much more modest (Figure 7G). Fenobam treatment in WT animals did shift the synapse population to a more WT distribution in layer 5 but not in layer 4 (Figures 7D and 7H). This again reaffirms the differences in the population response to fenobam of synapses in both layers.

To verify the fidelity of the regression it is important to show that the regression function can accurately categorize new data based on its animal background. We demonstrated this

by applying the regression function to 23,448 WT and 21,160 KO synapses from a pair of KO/WT animals that were randomly excluded from building the regression function. The correct categorization of these naive synapse populations by the regression clearly demonstrates that by synaptic molecular features alone the animal background of the imaged tissue can be diagnosed (Figures S6A and S6B). This not only validates the fidelity of the regression but also suggests that it is possible to diagnose the disease phenotype of a biopsy-size, sub-cubic millimeter piece of cortex based solely on its synapse protein metrics.

Finally, looking at the measures that the regression found most informative in determining whether a synapse is KO or WT, it is clear that the volume and distance of punctum from PSD measures are the most informative (Figure S6C; Table S1). This suggests that the size distribution of the synapse population in the KO animals is different from WT, which is an interesting observation in that the prevailing idea of FXS synapse dysfunction involves abnormal synapse plasticity and maturation (Comery et al., 1997; Dölen et al., 2007; Galvez and Greenough, 2005; Huber et al., 2002; Nimchinsky et al., 2001), which, if it is pervasive, should lead to system-level synapse size changes.

Regression Analysis of Synapse Classes Reveals Circuit-Specific Efficacy of Fenobam

Regression statistics can be generated on a synapse class level. This analysis confirms that layer 5 synapse molecular properties are more perturbed by FMRP loss than layer 4 synapse properties (Figure 8A). Fenobam treatment is also again more effective in layer 5 than in layer 4 (Figures 8A and 8B). Interestingly, VGluT1 synapse classes are more responsive to fenobam treatment than VGluT2 synapse classes (Figures 8A and 8B), and this is especially apparent in layer 4 (Figure 8B). Furthermore, in layer 4, this class-specific regression analysis reveals that synapses that contain FXR2P appear more WT than synapses that do not (Figures 8A and 8B), supporting the well-documented worsening of behavioral phenotypes in FXR2P and FMRP double KOs (Spencer et al., 2006; Tamanini et al., 1999; Zhang et al., 2009), and indicates that FXR2P can compensate in part the loss of FMRP. These results further reaffirm that synapse populations differentially respond to global perturbations such as FMRP loss or drug treatment. They demonstrate that this type of analysis can quantitatively reveal the class-specific efficacy of therapeutic compounds and that synapse specific analysis has the potential for assessing often complex response of the synapse population in diseases and its attempted treatment.

DISCUSSION

Hypothesized etiologies of mental and neurological disorders often involve abnormalities of molecular synapse phenotypes, but technical limitations have greatly restricted previous efforts to test such hypotheses directly and quantitatively. In particular, the heterogeneity of synapse populations in the mammalian CNS demands that decisive analysis be carried out at the level of individual synapses or individual synapse classes (Grant, 2012; O'Rourke et al., 2012). Unfortunately, the small size and dense intermixture of diverse synapse populations has resisted such analysis. Here we demonstrate the use of a unique approach to single-synapse analysis, based on AT and statistical image analysis methods, to explore synapse

abnormalities in a mouse model of human fragile X syndrome and to assess differential impacts of a candidate therapeutic compound on these synapse subsets.

The work described in this paper reveals that synapse phenotypes associated with FMRP loss are diversified by cortical layer, circuit type, and molecular composition of synapses. We show that cellular level changes of proteins can fail to reflect changes in levels of that same protein as measured in synapses. This suggests that synapse level analysis is essential for the determination of molecular changes in synapses in response to tissue-level perturbation. For example, the increase in layer 4 VGluT2 synapse density in *FMR1* KO animals is independent of total VGluT2 protein levels, and the overall decrease in cellular SYNPO protein level does not affect the density of synapses that contain SYNPO. These data demonstrate that measuring synaptic protein changes in response to system-level perturbations requires single synapse analysis.

The broad scope of our data combined with the synaptic and circuit-level analysis afford us a unique perspective on diverse mechanisms that affect synapse change in response to global FMRP loss. For instance, the observations that layer 5 synapse protein properties in *Fmr1* KO are highly perturbed while layer 5 synapse density is essentially unchanged coupled with the opposite observations in layer 4 suggest different population-level mechanisms acting in the two layers in response to the loss of FMRP. Layer 4 circuits appear to engage circuit level plasticity by increasing the number of synaptic contacts, leaving individual synapses more similar to WT, while layer 5 circuits appear to engage synapse-level plasticity, thus altering synaptic protein properties without significantly modulating the number of synaptic contacts. Another example is the responsiveness of the GABA system to glutamatergic synapse density change. GABAergic synapses were elevated in the KO, which maintained the WT GABAergic to glutamatergic synapse density ratio. Fenobam, a glutamate receptor antagonist that rescues glutamate synapse density changes in the KO, is also able to rescue GABAergic synapse density changes. These data are consistent with the allosteric regulation of GABA transmission by changes in glutamate signaling, even though we cannot fully discount the direct action of mGluR5 on GABAergic synapses.

Our data also reveal that global loss of FMRP does not affect all cortical layers and synaptic circuits similarly. We show that there is an increase in thalamic synapses in layer 4 of *Fmr1* KO animals, while there is a decrease in layer 5 thalamic synapse density in the KO. This suggests a change in the balance of thalamocortical input into the cortex, which could be mediated by either local changes in synapse density or long-range wiring deficits. Meanwhile, layer 5 VGluT2-containing thalamic synapses are more perturbed, as measured by molecular features, than layer 4 thalamic synapses. This further suggests that layer 5 thalamic input is more affected by FMRP loss than layer 4 thalamic input, which is interesting in light of recent findings that suggest layer 5 thalamocortical input represents a more direct path of information transmission from the sensory modalities through the cortex by bypassing the tradition model of columnar cortical information processing (Constantinople and Bruno, 2013). This suggests that this mode of direct information transmission might be more degraded in *Fmr1* KO mice and perhaps in FXS patients as well. This represents a potential mechanism for sensory information processing deficits caused by FMRP loss that requires further investigation.

The resistance of thalamocortical VGluT2-containing synapses to fenobam treatment, as revealed by the regression analysis, coupled with the knowledge that thalamic neurons selectively express FMRP in axon terminals (Akins et al., 2012; Christie et al., 2009) and that this presynaptic FMRP expression is enriched in development (Akins et al., 2012) suggest a role in which FMRP affects the guidance and wiring of thalamic axons (Christie et al., 2009). Thus, FMRP loss during development might cause a wiring deficit in the thalamocortical circuits that are insensitive to the postdevelopmental application of fenobam, as was revealed by our data. Moreover, it is important to note that this current study, while extensive in its synaptic coverage, is only a snapshot in time of adult (4 month) somatosensory cortex. We know that during development there are critical periods during which the connectivity of the brain is irrevocably altered. FMRP loss is lifelong; thus, one would expect there to be a buildup of connectivity abnormalities imprinted by direct and compensatory mechanisms during these critical periods. This suggests that there may be time-dependent therapeutic windows and long-range, brain-wide wiring deficits in *Fmr1* KO mice that are currently unknown.

Thus, large-scale, single-synapse analysis demonstrates the extraordinary complexity and diversity in responses to FMRP loss. The quantification of the complex nature of synaptic changes in FXS illustrates the difficulty in designing treatments for neurodevelopmental disorders, as any rescue attempted beyond the initial perturbation (FMRP loss), such as mGluR5 antagonism, immediately becomes a process of dealing with a cascade of direct and indirect molecular interactions. It is in this complex interaction of cells and molecules that the type of physiologically grounded, phenotype-based analysis presented in this paper become invaluable, as it provides a method for quantifying the complex system-level response of the nervous system to brain-wide perturbations.

Moreover, the demonstration that FXS, a monogenic disorder, causes a highly diverse set of synaptic phenotypes suggests that other cognitive disorders with still more complex genetic and environmental etiologies (such autism spectrum, neurodegenerative, and psychiatric disorders) are also likely to possess a diverse range of molecular abnormalities across synapse populations. More importantly, these data demonstrate that synapses are not all the same. Molecular and physiological mechanisms discovered in one cell type, in one region of the brain, do not necessarily generalize across all cells in the brain. Diseases, as well as pharmaceuticals, will have differential impacts on cells and synapses dependent upon the location and identity of their cellular neighborhoods. Thus, it is important, moving forward, to understand neurological diseases and their treatment in terms of how cellular systems interact across circuits and regions on a molecular level.

EXPERIMENTAL PROCEDURES

Preparation of AT Ribbon Arrays and Immunohistochemistry

Tissue preparation, array creation, and immunohistochemistry are described in detail in previous publications (Micheva and Smith, 2007).

Primary Antibodies

For a detailed discussion of the antibodies used in this study and the vetting of those antibodies, see the Supplemental Experimental Procedures.

Microscopy

Wide-field imaging of ribbons were accomplished on a *Zeiss* Axio Imager.Z1 Upright Fluorescence Microscope with motorized stage and Axiocam HR Digital Camera, as previously described (Wang and Smith, 2012). A position list was generated for each ribbon array of ultrathin sections using custom software modules written for Axiovision. Single fields of view were imaged for each position in the position list using a *Zeiss* 63×/1.4 NA Plan Apochromat objective.

Image Registration and Computational Processing

AT data matrixes were registered and analyzed through a combination of FIJI plug-ins and proprietary Matlab (*Mathworks*) functions (for a detailed description of the computational pipeline, see Supplemental Experimental Procedures).

Regression Analysis and Statistics

Regression analyses and significance statistics were performed using a combination of Matlab native functions and custom scripts (see Supplemental Experimental Procedures). Multiple comparison errors in p values are controlled via Benjamini-Hochberg false discovery rate correction in Matlab using third party developed functions (see Supplemental Experimental Procedures).

Drug Treatment

Male 4 month of age, FMRP KO mice (C57BL/6) and WT mice were fed fenobam-supplemented food (100 mg fenobam/kg body weight) on a daily basis for two weeks. After two weeks the animals were sacrificed and the brains were prepared for array tomography. Animals were housed and handled in accordance with protocols approved by the Administrative Panel on Laboratory Animal Care (APLAC) of Stanford University.

ACKNOWLEDGMENTS

We thank Drs. Ben Barres, Michael Tranfaglia, Kimberley McAllister, William DeBello, Joachim Hallmayer, Logan Grosenick, Louis Leung, Kristina Micheva, Dan Madison, and Michael Tadross for helpful discussion and edits on the manuscript. We thank FRAXA foundation and Dr. Michael Tranfaglia for providing access to fenobam. We thank Drs. Yi Zuo and Xinzhu Yu for providing the FXS KO mice for the experiments. We thank Drs. Jeffrey D. Rothstein, Justin Fallon, and Rob Willemsen for providing antibodies. We thank Gemini Skariah and Nafisa Ghori for their technical help. G.X.W. was supported in part by a postdoctoral fellowship from FRAXA foundation. This work was supported by grants from the Gatsby Charitable Trust, the Howard Hughes Medical Institute (Collaborative Innovation Award #43667), the Mathers Foundation, and grants from the National Institute of Health (NS062798, DK090065, MH099647, NS077601, and MH099797). S.S. has equity in Aratome, a company dedicated to the commercialization of AT.

REFERENCES

Adams-Cioaba MA, Guo Y, Bian C, Amaya MF, Lam R, Wasney GA, Vedadi M, Xu C, Min J. Structural studies of the tandem Tudor domains of fragile X mental retardation related proteins FXR1 and FXR2. PLoS ONE. 2010; 5:e13559. [PubMed: 21072162]

Adusei DC, Pacey LKK, Chen D, Hampson DR. Early developmental alterations in GABAergic protein expression in fragile X knockout mice. Neuropharmacology. 2010; 59:167–171. [PubMed: 20470805]

Akins MR, Leblanc HF, Stackpole EE, Chyung E, Fallon JR. Systematic mapping of fragile X granules in the mouse brain reveals a potential role for presynaptic FMRP in sensorimotor functions. J. Comp. Neurol. 2012; 520:3687–3706. [PubMed: 22522693]

Anwyl R. Metabotropic glutamate receptor-dependent long-term potentiation. Neuropharmacology. 2009; 56:735–740. [PubMed: 19705571]

Aronoff R, Matyas F, Mateo C, Ciron C, Schneider B, Petersen CCH. Long-range connectivity of mouse primary somatosensory barrel cortex. Eur. J. Neurosci. 2010; 31:2221–2233. [PubMed: 20550566]

Auerbach BD, Osterweil EK, Bear MF. Mutations causing syndromic autism define an axis of synaptic pathophysiology. Nature. 2011; 480:63–68. [PubMed: 22113615]

Baranek GT, Roberts JE, David FJ, Sideris J, Mirrett PL, Hatton DD, Bailey DB Jr. Developmental trajectories and correlates of sensory processing in young boys with fragile X syndrome. Phys. Occup. Ther. Pediatr. 2008; 28:79–98. [PubMed: 18399048]

Bayés A, van de Lagemaat LN, Collins MO, Croning MDR, Whittle IR, Choudhary JS, Grant SGN. Characterization of the proteome, diseases and evolution of the human postsynaptic density. Nat. Neurosci. 2011; 14:19–21. [PubMed: 21170055]

Berry-Kravis E, Hessl D, Coffey S, Hervey C, Schneider A, Yuhas J, Hutchison J, Snape M, Tranfaglia M, Nguyen DV, Hagerman R. A pilot open label, single dose trial of fenobam in adults with fragile X syndrome. J. Med. Genet. 2009; 46:266–271. [PubMed: 19126569]

Berry-Kravis EM, Hessl D, Rathmell B, Zarevics P, Cherubini M, Walton-Bowen K, Mu Y, Nguyen DV, Gonzalez-Heydrich J, Wang PP, et al. Effects of STX209 (arbaclofen) on neurobehavioral function in children and adults with fragile X syndrome: a randomized, controlled, phase 2 trial. Sci. Transl. Med. 2012; 4:ra127.

Bhakar AL, Dölen G, Bear MF. The pathophysiology of fragile X (and what it teaches us about synapses). Annu. Rev. Neurosci. 2012; 35:417–443. [PubMed: 22483044]

Ceman S, Brown V, Warren ST. Isolation of an FMRP-associated messenger ribonucleoprotein particle and identification of nucleolin and the fragile X-related proteins as components of the complex. Mol. Cell. Biol. 1999; 19:7925–7932. [PubMed: 10567518]

Chen X, Winters C, Azzam R, Li X, Galbraith JA, Leapman RD, Reese TS. Organization of the core structure of the postsynaptic density. Proc. Natl. Acad. Sci. USA. 2008; 105:4453–4458. [PubMed: 18326622]

Christie SB, Akins MR, Schwob JE, Fallon JR. The FXG: a presynaptic fragile X granule expressed in a subset of developing brain circuits. J. Neurosci. 2009; 29:1514–1524. [PubMed: 19193898]

Coghlan S, Horder J, Inkster B, Mendez MA, Murphy DG, Nutt DJ. GABA system dysfunction in autism and related disorders: from synapse to symptoms. Neurosci. Biobehav. Rev. 2012; 36:2044–2055. [PubMed: 22841562]

Comery TA, Harris JB, Willems PJ, Oostra BA, Irwin SA, Weiler IJ, Greenough WT. Abnormal dendritic spines in fragile X knockout mice: maturation and pruning deficits. Proc. Natl. Acad. Sci. USA. 1997; 94:5401–5404. [PubMed: 9144249]

Constantinople CM, Bruno RM. Deep cortical layers are activated directly by thalamus. Science. 2013; 340:1591–1594. [PubMed: 23812718]

Cruz-Martín A, Crespo M, Portera-Cailliau C. Delayed stabilization of dendritic spines in fragile X mice. J. Neurosci. 2010; 30:7793–7803. [PubMed: 20534828]

Cruz-Martín A, Crespo M, Portera-Cailliau C. Glutamate induces the elongation of early dendritic protrusions via mGluRs in wild type mice, but not in fragile X mice. PLoS ONE. 2012; 7:e32446. [PubMed: 22384253]

Cummings JL, Banks SJ, Gary RK, Kinney JW, Lombardo JM, Walsh RR, Zhong K. Alzheimer's disease drug development: translational neuroscience strategies. CNS Spectr. 2013; 18:128–138. [PubMed: 23472637]

D'Hulst C, Heulens I, Brouwer JR, Willemsen R, De Geest N, Reeve SP, De Deyn PP, Hassan BA, Kooy RF. Expression of the GABAergic system in animal models for fragile X syndrome and

fragile X associated tremor/ataxia syndrome (FXTAS). Brain Res. 2009; 1253:176–183. [PubMed: 19070606]

De Camilli P, Harris SM Jr, Huttner WB, Greengard P. Synapsin I (Protein I), a nerve terminal-specific phosphoprotein. II. Its specific association with synaptic vesicles demonstrated by immunocytochemistry in agarose-embedded synaptosomes. J. Cell Biol. 1983; 96:1355–1373. [PubMed: 6404911]

de Vrij FMS, Levenga J, van der Linde HC, Koekkoek SK, De Zeeuw CI, Nelson DL, Oostra BA, Willemsen R. Rescue of behavioral phenotype and neuronal protrusion morphology in Fmr1 KO mice. Neurobiol. Dis. 2008; 31:127–132. [PubMed: 18571098]

Defelipe J. The evolution of the brain, the human nature of cortical circuits, and intellectual creativity. Front Neuroanat. 2011; 5:29. [PubMed: 21647212]

Deller T, Merten T, Roth SU, Mundel P, Frotscher M. Actin-associated protein synaptopodin in the rat hippocampal formation: localization in the spine neck and close association with the spine apparatus of principal neurons. J. Comp. Neurol. 2000; 418:164–181. [PubMed: 10701442]

Deller T, Korte M, Chabanis S, Drakew A, Schwegler H, Stefani GG, Zuniga A, Schwarz K, Bonhoeffer T, Zeller R, et al. Synaptopodin-deficient mice lack a spine apparatus and show deficits in synaptic plasticity. Proc. Natl. Acad. Sci. USA. 2003; 100:10494–10499. [PubMed: 12928494]

Dölen G, Bear MF. Role for metabotropic glutamate receptor 5 (mGluR5) in the pathogenesis of fragile X syndrome. J. Physiol. 2008; 586:1503–1508. [PubMed: 18202092]

Dölen G, Osterweil E, Rao BSS, Smith GB, Auerbach BD, Chattarji S, Bear MF. Correction of fragile X syndrome in mice. Neuron. 2007; 56:955–962. [PubMed: 18093519]

Dölen G, Carpenter RL, Ocain TD, Bear MF. Mechanism-based approaches to treating fragile X. Pharmacol. Ther. 2010; 127:78–93. [PubMed: 20303363]

Douglas RJ, Martin KAC. Neuronal circuits of the neocortex. Annu. Rev. Neurosci. 2004; 27:419–451. [PubMed: 15217339]

El Idrissi A, Ding X-H, Scalia J, Trenkner E, Brown WT, Dobkin C. Decreased GABA(A) receptor expression in the seizure-prone fragile X mouse. Neurosci. Lett. 2005; 377:141–146. [PubMed: 15755515]

Emes RD, Grant SGN. Evolution of synapse complexity and diversity. Annu. Rev. Neurosci. 2012; 35:111–131. [PubMed: 22715880]

Feldmeyer D, Sakmann B. Synaptic efficacy and reliability of excitatory connections between the principal neurones of the input (layer 4) and output layer (layer 5) of the neocortex. J. Physiol. 2000; 525:31–39. [PubMed: 10811722]

Fremeau RT Jr, Troyer MD, Pahner I, Nygaard GO, Tran CH, Reimer RJ, Bellocchio EE, Fortin D, Storm-Mathisen J, Edwards RH. The expression of vesicular glutamate transporters defines two classes of excitatory synapse. Neuron. 2001; 31:247–260. [PubMed: 11502256]

Gallagher SM, Daly CA, Bear MF, Huber KM. Extracellular signal-regulated protein kinase activation is required for metabotropic glutamate receptor-dependent long-term depression in hippocampal area CA1. J. Neurosci. 2004; 24:4859–4864. [PubMed: 15152046]

Galvez R, Greenough WT. Sequence of abnormal dendritic spine development in primary somatosensory cortex of a mouse model of the fragile X mental retardation syndrome. Am. J. Med. Genet A. 2005; 135:155–160. [PubMed: 15880753]

Galvez R, Gopal AR, Greenough WT. Somatosensory cortical barrel dendritic abnormalities in a mouse model of the fragile X mental retardation syndrome. Brain Res. 2003; 971:83–89. [PubMed: 12691840]

Garden GA, La Spada AR. Intercellular (mis)communication in neurodegenerative disease. Neuron. 2012; 73:886–901. [PubMed: 22405200]

Gibson JR, Bartley AF, Hays SA, Huber KM. Imbalance of neocortical excitation and inhibition and altered UP states reflect network hyperexcitability in the mouse model of fragile X syndrome. J. Neurophysiol. 2008; 100:2615–2626. [PubMed: 18784272]

Grant SGN. Synaptopathies: diseases of the synaptome. Curr. Opin. Neurobiol. 2012; 22:522–529. [PubMed: 22409856]

Graziano A, Liu X-B, Murray KD, Jones EG. Vesicular glutamate transporters define two sets of glutamatergic afferents to the somatosensory thalamus and two thalamocortical projections in the mouse. J. Comp. Neurol. 2008; 507:1258–1276. [PubMed: 18181146]

Grewal SS, York RD, Stork PJ. Extracellular-signal-regulated kinase signalling in neurons. Curr. Opin. Neurobiol. 1999; 9:544–553. [PubMed: 10508738]

Henderson VC, Kimmelman J, Fergusson D, Grimshaw JM, Hackam DG. Threats to validity in the design and conduct of preclinical efficacy studies: a systematic review of guidelines for in vivo animal experiments. PLoS Med. 2013; 10:e1001489. [PubMed: 23935460]

Herzog E, Bellenchi GC, Gras C, Bernard V, Ravassard P, Bedet C, Gasnier B, Giros B, El Mestikawy S. The existence of a second vesicular glutamate transporter specifies subpopulations of glutamatergic neurons. J. Neurosci. 2001; 21:RC181. [PubMed: 11698619]

Heuser, JE.; Reese, TS. Structure of the synapse. In: Kandall, ER., editor. Handbook of Physiology I: The Nervous System. Oxford: Oxford University Press; 1977. p. 261-294.

Hoeffer CA, Klann E. mTOR signaling: at the crossroads of plasticity, memory and disease. Trends Neurosci. 2010; 33:67–75. [PubMed: 19963289]

Hoeft F, Carter JC, Lightbody AA, Cody Hazlett H, Piven J, Reiss AL. Region-specific alterations in brain development in one- to three-year-old boys with fragile X syndrome. Proc. Natl. Acad. Sci. USA. 2010; 107:9335–9339. [PubMed: 20439717]

Holbro N, Grunditz A, Oertner TG. Differential distribution of endoplasmic reticulum controls metabotropic signaling and plasticity at hippocampal synapses. Proc. Natl. Acad. Sci. USA. 2009; 106:15055–15060. [PubMed: 19706463]

Hosmer, DW.; Lemeshow, S. Applied Logistic Regression in Wiley Series in Probability and Statistics. Hoboken: John Wiley & Sons, Inc.; 2000.

Hu J-H, Park JM, Park S, Xiao B, Dehoff MH, Kim S, Hayashi T, Schwarz MK, Huganir RL, Seeburg PH, et al. Homeostatic scaling requires group I mGluR activation mediated by Homer1a. Neuron. 2010; 68:1128–1142. [PubMed: 21172614]

Huber KM, Kayser MS, Bear MF. Role for rapid dendritic protein synthesis in hippocampal mGluR-dependent long-term depression. Science. 2000; 288:1254–1257. [PubMed: 10818003]

Huber KM, Gallagher SM, Warren ST, Bear MF. Altered synaptic plasticity in a mouse model of fragile X mental retardation. Proc. Natl. Acad. Sci. USA. 2002; 99:7746–7750. [PubMed: 12032354]

Hunt CA, Schenker LJ, Kennedy MB. PSD-95 is associated with the postsynaptic density and not with the presynaptic membrane at forebrain synapses. J. Neurosci. 1996; 16:1380–1388. [PubMed: 8778289]

Kaneko T, Fujiyama F. Complementary distribution of vesicular glutamate transporters in the central nervous system. Neurosci. Res. 2002; 42:243–250. [PubMed: 11985876]

Kindler S, Kreienkamp H-J. Dendritic mRNA targeting and translation. Adv. Exp. Med. Biol. 2012; 970:285–305. [PubMed: 22351061]

Kogan CS, Boutet I, Cornish K, Zangenehpour S, Mullen KT, Holden JJA, Der Kaloustian VM, Andermann E, Chaudhuri A. Differential impact of the FMR1 gene on visual processing in fragile X syndrome. Brain. 2004; 127:591–601. [PubMed: 14736752]

Lauterborn JC, Jafari M, Babayan AH, Gall CM. Environmental enrichment reveals effects of genotype on hippocampal spine morphologies in the mouse model of fragile X syndrome. Cereb. Cortex. 2013 http://dx.doi.org/10.1093/cercor/bht249.

Le Duigou C, Holden T, Kullmann DM. Short- and long-term depression at glutamatergic synapses on hippocampal interneurons by group I mGluR activation. Neuropharmacology. 2011; 60:748–756. [PubMed: 21185314]

Li P, Rudolph U, Huntsman MM. Long-term sensory deprivation selectively rearranges functional inhibitory circuits in mouse barrel cortex. Proc. Natl. Acad. Sci. USA. 2009; 106:12156–12161. [PubMed: 19584253]

Lübke J, Feldmeyer D. Excitatory signal flow and connectivity in a cortical column: focus on barrel cortex. Brain Struct. Funct. 2007; 212:3–17. [PubMed: 17717695]

Maffei A, Nataraj K, Nelson SB, Turrigiano GG. Potentiation of cortical inhibition by visual deprivation. Nature. 2006; 443:81–84. [PubMed: 16929304]

Michalon A, Sidorov M, Ballard TM, Ozmen L, Spooren W, Wettstein JG, Jaeschke G, Bear MF, Lindemann L. Chronic pharmacological mGlu5 inhibition corrects fragile X in adult mice. Neuron. 2012; 74:49–56. [PubMed: 22500629]

Micheva KD, Beaulieu C. An anatomical substrate for experience- dependent plasticity of the rat barrel field cortex. Proc. Natl. Acad. Sci. USA. 1995; 92:11834–11838. [PubMed: 8524859]

Micheva KD, Smith SJ. Array tomography: a new tool for imaging the molecular architecture and ultrastructure of neural circuits. Neuron. 2007; 55:25–36. [PubMed: 17610815]

Micheva KD, Busse B, Weiler NC, O'Rourke N, Smith SJ. Single-synapse analysis of a diverse synapse population: proteomic imaging methods and markers. Neuron. 2010; 68:639–653. [PubMed: 21092855]

Nahmani M, Erisir A. VGluT2 immunochemistry identifies thalamocortical terminals in layer 4 of adult and developing visual cortex. J. Comp. Neurol. 2005; 484:458–473. [PubMed: 15770654]

Nakamura K, Hioki H, Fujiyama F, Kaneko T. Postnatal changes of vesicular glutamate transporter (VGluT)1 and VGluT2 immunoreactivities and their colocalization in the mouse forebrain. J. Comp. Neurol. 2005; 492:263–288. [PubMed: 16217795]

Nimchinsky EA, Oberlander AM, Svoboda K. Abnormal development of dendritic spines in FMR1 knock-out mice. J. Neurosci. 2001; 21:5139–5146. [PubMed: 11438589]

Nimchinsky EA, Sabatini BL, Svoboda K. Structure and function of dendritic spines. Annu. Rev. Physiol. 2002; 64:313–353. [PubMed: 11826272]

O'Rourke NA, Weiler NC, Micheva KD, Smith SJ. Deep molecular diversity of mammalian synapses: why it matters and how to measure it. Nat. Rev. Neurosci. 2012; 13:365–379. [PubMed: 22573027]

Osterweil EK, Chuang S-C, Chubykin AA, Sidorov M, Bianchi R, Wong RKS, Bear MF. Lovastatin corrects excess protein synthesis and prevents epileptogenesis in a mouse model of fragile X syndrome. Neuron. 2013; 77:243–250. [PubMed: 23352161]

Pieretti M, Zhang FP, Fu YH, Warren ST, Oostra BA, Caskey CT, Nelson DL. Absence of expression of the FMR-1 gene in fragile X syndrome. Cell. 1991; 66:817–822. [PubMed: 1878973]

Robertson L. mGlu5 as a potential therapeutic target for the treatment of fragile X syndrome. Biosci. Horizons. 2013; 6 http://dx.doi.org/10.1093/biohorizons/hzt001.

Schubert D, Kötter R, Staiger JF. Mapping functional connectivity in barrel-related columns reveals layer- and cell type-specific microcircuits. Brain Struct. Funct. 2007; 212:107–119. [PubMed: 17717691]

Segal M. Dendritic spines and long-term plasticity. Nat. Rev. Neurosci. 2005; 6:277–284. [PubMed: 15803159]

Segal M, Vlachos A, Korkotian E. The spine apparatus, synaptopodin, and dendritic spine plasticity. Neuroscientist. 2010; 16:125–131. [PubMed: 20400711]

Sharma A, Hoeffer CA, Takayasu Y, Miyawaki T, McBride SM, Klann E, Zukin RS. Dysregulation of mTOR signaling in fragile X syndrome. J. Neurosci. 2010; 30:694–702. [PubMed: 20071534]

Sheng M, Sabatini BL, Südhof TC. Synapses and Alzheimer's disease. Cold Spring Harb. Perspect. Biol. 2012; 4 http://dx.doi.org/10.1016/j.neuropharm.2013.03.030.

Shiflett MW, Balleine BW. Contributions of ERK signaling in the striatum to instrumental learning and performance. Behav. Brain Res. 2011; 218:240–247. [PubMed: 21147168]

Spencer CM, Serysheva E, Yuva-Paylor LA, Oostra BA, Nelson DL, Paylor R. Exaggerated behavioral phenotypes in Fmr1/Fxr2 double knockout mice reveal a functional genetic interaction between Fragile X-related proteins. Hum. Mol. Genet. 2006; 15:1984–1994. [PubMed: 16675531]

Sweatt JD. The neuronal MAP kinase cascade: a biochemical signal integration system subserving synaptic plasticity and memory. J. Neurochem. 2001; 76:1–10. [PubMed: 11145972]

Tada T, Sheng M. Molecular mechanisms of dendritic spine morphogenesis. Curr. Opin. Neurobiol. 2006; 16:95–101. [PubMed: 16361095]

Tamanini F, Willemsen R, van Unen L, Bontekoe C, Galjaard H, Oostra BA, Hoogeveen AT. Differential expression of FMR1, FXR1 and FXR2 proteins in human brain and testis. Hum. Mol. Genet. 1997; 6:1315–1322. [PubMed: 9259278]

Tamanini F, Van Unen L, Bakker C, Sacchi N, Galjaard H, Oostra BA, Hoogeveen AT. Oligomerization properties of fragile-X mental-retardation protein (FMRP) and the fragile-X-related proteins FXR1P and FXR2P. Biochem. J. 1999; 343:517–523. [PubMed: 10527928]

Thiels E, Klann E. Extracellular signal-regulated kinase, synaptic plasticity, and memory. Rev. Neurosci. 2001; 12:327–345. [PubMed: 11783718]

Till SM, Wijetunge LS, Seidel VG, Harlow E, Wright AK, Bagni C, Contractor A, Gillingwater TH, Kind PC. Altered maturation of the primary somatosensory cortex in a mouse model of fragile X syndrome. Hum. Mol. Genet. 2012; 21:2143–2156. [PubMed: 22328088]

Tsanov M, Manahan-Vaughan D. Synaptic plasticity in the adult visual cortex is regulated by the metabotropic glutamate receptor, mGluR5. Exp. Brain Res. 2009; 199:391–399. [PubMed: 19672584]

Ueta Y, Yamamoto R, Sugiura S, Inokuchi K, Kato N. Homer 1a suppresses neocortex long-term depression in a cortical layer-specific manner. J. Neurophysiol. 2008; 99:950–957. [PubMed: 18077661]

Ventura R, Pascucci T, Catania MV, Musumeci SA, Puglisi-Allegra S. Object recognition impairment in Fmr1 knockout mice is reversed by amphetamine: involvement of dopamine in the medial prefrontal cortex. Behav. Pharmacol. 2004; 15:433–442. [PubMed: 15343070]

Verkerk AJ, Pieretti M, Sutcliffe JS, Fu YH, Kuhl DP, Pizzuti A, Reiner O, Richards S, Victoria MF, Zhang FP, et al. Identification of a gene (FMR-1) containing a CGG repeat coincident with a breakpoint cluster region exhibiting length variation in fragile X syndrome. Cell. 1991; 65:905–914. [PubMed: 1710175]

Vinueza Veloz MF, Buijsen RAM, Willemsen R, Cupido A, Bosman LWJ, Koekkoek SKE, Potters JW, Oostra BA, De Zeeuw CI. The effect of an mGluR5 inhibitor on procedural memory and avoidance discrimination impairments in Fmr1 KO mice. Genes Brain Behav. 2012; 11:325–331. [PubMed: 22257369]

Vlachos A, Korkotian E, Schonfeld E, Copanaki E, Deller T, Segal M. Synaptopodin regulates plasticity of dendritic spines in hippocampal neurons. J. Neurosci. 2009; 29:1017–1033. [PubMed: 19176811]

Wang G, Smith SJ. Sub-diffraction limit localization of proteins in volumetric space using Bayesian restoration of fluorescence images from ultrathin specimens. PLoS Comput. Biol. 2012; 8:e1002671. [PubMed: 22956902]

Wijetunge LS, Till SM, Gillingwater TH, Ingham CA, Kind PC. mGluR5 regulates glutamate-dependent development of the mouse somatosensory cortex. J. Neurosci. 2008; 28:13028–13037. [PubMed: 19052194]

Wijetunge LS, Angibaud J, Frick A, Kind PC, Nägerl UV. Stimulated emission depletion (STED) microscopy reveals nanoscale defects in the developmental trajectory of dendritic spine morphogenesis in a mouse model of fragile X syndrome. J. Neurosci. 2014; 34:6405–6412. [PubMed: 24790210]

Yan QJ, Asafo-Adjei PK, Arnold HM, Brown RE, Bauchwitz RP. A phenotypic and molecular characterization of the fmr1-tm1Cgr fragile X mouse. Genes Brain Behav. 2004; 3:337–359. [PubMed: 15544577]

Yuste R, Bonhoeffer T. Morphological changes in dendritic spines associated with long-term synaptic plasticity. Annu. Rev. Neurosci. 2001; 24:1071–1089. [PubMed: 11520928]

Zhang L, Alger BE. Enhanced endocannabinoid signaling elevates neuronal excitability in fragile X syndrome. J. Neurosci. 2010; 30:5724–5729. [PubMed: 20410124]

Zhang J, Hou L, Klann E, Nelson DL. Altered hippocampal synaptic plasticity in the FMR1 gene family knockout mouse models. J. Neurophysiol. 2009; 101:2572–2580. [PubMed: 19244359]

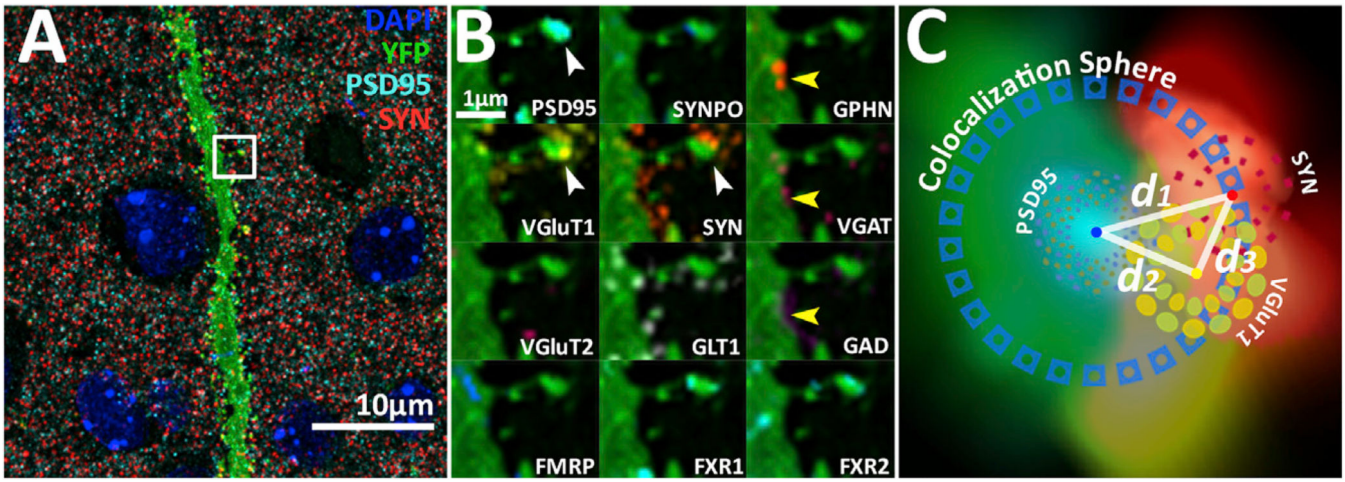

Figure 1. Detection and Classification of Synapses from Multichannel Array Tomographic Volume Images

(A) Composite maximum intensity projection illustrating the density of synaptic protein puncta in layer 4 cortex. Blue, DAPI; green, YFP; cyan, PSD95; red, SYN; and yellow, VGluT1. Scale bar, 10 µm. White arrowhead points at a dendritic spine with a glutamatergic VGluT1-containing synapse. Yellow arrowhead points at a dendrite shaft GABAergic synapse. Projected volume: 0.3 mm by 0.3 mm by 2 µm.

(B) Zoomed-in views of dendrite segment marked by white box in (A). Each box contains only one protein marker as labeled in the lower left of each box. Note the orientation of the synaptic markers, where postsynaptic and presynaptic molecules are spatially organized in a specific pattern. Also, note how the synapse present on the spine can be classified as a VGluT1 synapse based on the presence of VGluT1 and the absence of VGluT2.

(C) Schematic of distance calculations made for synapse analysis superimposed on 2D projection of a volumetric rendering of the excitatory synapse in ([B], white arrowhead). Distance between the center of mass from PSD95 and SYN (*d1*) is used to generate a colocalization sphere for the determination of protein colocalization (e.g., if the distance of a VGluT1 center to PSD95 [*d2*] is smaller than [*d1*], then that punctum is considered colocalized to the candidate synapse). The verification of the candidate synapse represented by the PSD95-to-SYN pair is made if the distance of the VGluT1 center to PSD95 (*d2*) is longer than the distance of the VGluT1 center to SYN (*d3*), signifying that the VGluT1 is presynaptic.

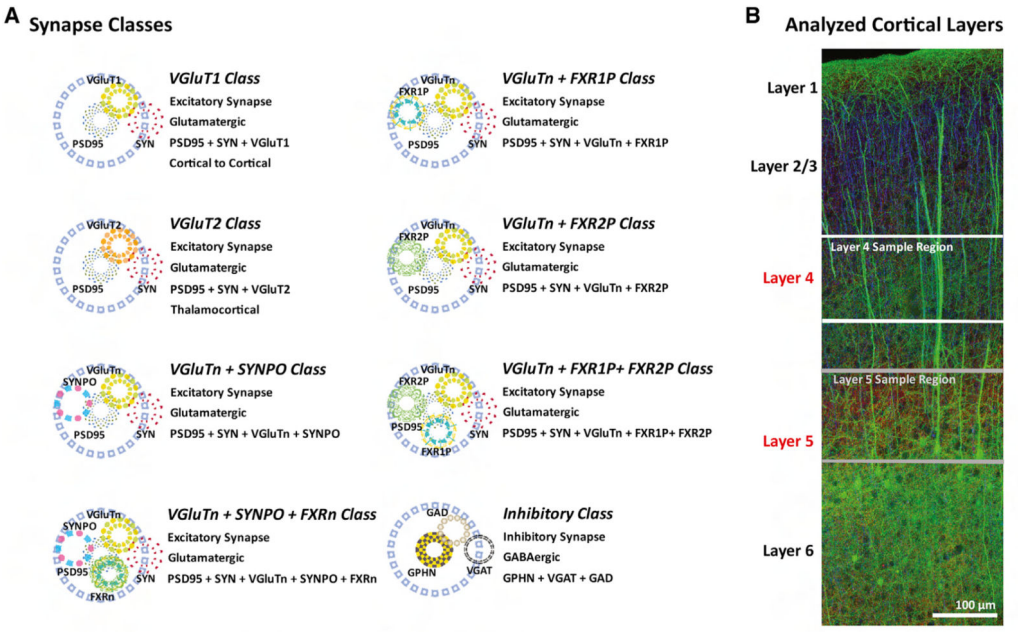

C

Proteins Targeted by Antibodies

Proteins discussed in this paper and their known synaptic function

Protein Name	Function Notes
Post-synaptic proteins in glutamatergic synapses	
Post-synaptic density protein 95 (PSD95)	Scaffolding protein in excitatory synapses
Post-synaptic proteins in GABAergic synapses	
Gephyrin (GPHN)	Scaffolding protein in inhibitory synapses
Dendritic proteins	
Synaptopodin (SYNPO)	Marker of the spine apparatus and mature spines
Presynaptic proteins in all synapses	
Synapsin (SYN)	Vesicle associated scaffolding protein
Presynaptic proteins in glutamatergic synapses	
Vesicular glutamate transporter 1 (VGluT1)	Vesicular Glu transporter in a subset of synapses
Vesicular glutamate transporter 2 (VGluT2)	Vesicular Glu transporter in a subset of synapses
Presynaptic proteins in GABAergic synapses	
Vesicular GABA transporter (VGAT)	Vesicular GABA transporter in all inhibitory synapses
Glutamate decarboxylase (GAD)	Enzyme that produces GABA from Glu
RNA binding proteins	
Fragile X mental retardation protein (FMRP)	RNA binding protein, inhibitor of RNA translation
Fragile X related protein 1 (FXR1P)	RNA binding protein, autosomal homologue of FMRP
Fragile X related protein 2 (FXR2P)	RNA binding protein, autosomal homologue of FMRP

Figure 2. Cortical Layers, Synapse Classes, and Synaptic Proteins Analyzed in This Study

(A) Schematic representation of synapse classes. Blue circle represent the colocalization sphere. VGluT*n*, VGluT1 and VGluT2. FXR*n*, FXR1 and FXR2.

(B) Cortical Layers 4 and 5 are selected for analysis because sensory processing deficits are important behavioral abnormalities seen in FXS. Image: YFP, green; acetylated tubulin, blue; and SYN, red.

(C) Table of proteins discussed in this paper and their known synaptic function.

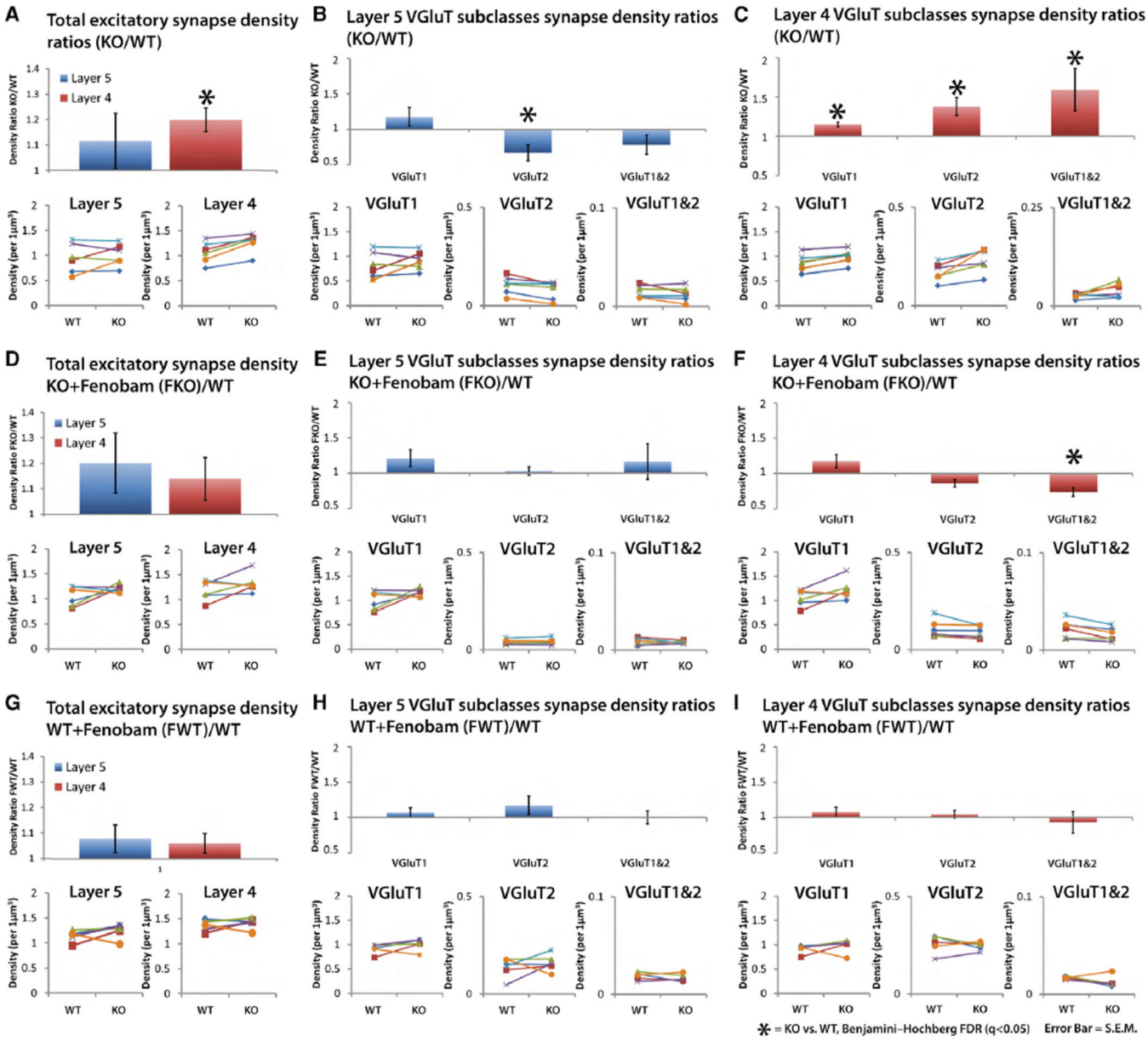

Figure 3. Density Comparison of Synapses Reveals Layer- and Class-Specific Response to FMRP Loss and Fenobam Treatment

(A–I) Average density ratio of KO versus WT synapses from paired mice tissue (see Experimental Procedures). Paired tissue is used to reduce variability in tissue processing and immunolabeling.

(A) Density ratios of KO/WT for the total excitatory synapse population in layers 5 and 4. Layer 4 synapse density is increased in the KO, but in not layer 5. (Insets) The densities of each individual KO/WT pairs are plotted (n = 6 pairs).

(B) Density ratios for layer 5 VGluT synapse classes and their plotted individual densities. There is a specific decrease in VGluT2 synapse density in layer 5.

(C) Density ratios for layer 4 VGluT synapse classes and their plotted individual densities. Synapse density is increased in all classes.

(D) Density ratios of fenobam-treated KO (FKO)/WT for the total excitatory synapse population in layers 5 and 4 (n = 6 pairs). Fenobam rescues layer 4 density increases in KO.
(E) Density ratios (FKO/WT) of layer 5 VGluT synapse classes. Fenobam normalizes the specific VGluT2 synapse density increase in layer 5.
(F) Density ratios of Layer 4 VGluT synapse classes. Fenobam normalizes density increases, except for VGluT1 and 2 class synapses.
(G–I) Density ratios of fenobam-treated WT (FWT)/WT for the total excitatory synapse population in layers 5 and 4 (n = 5 pairs). Fenobam does not induce significant change in synapse density in the WT. Error bars, SE. Significance is calculated using paired t tests, and the p values are adjusted via Benjamini-Hochberg false discovery rate (FDR) test. $q < 0.05$.

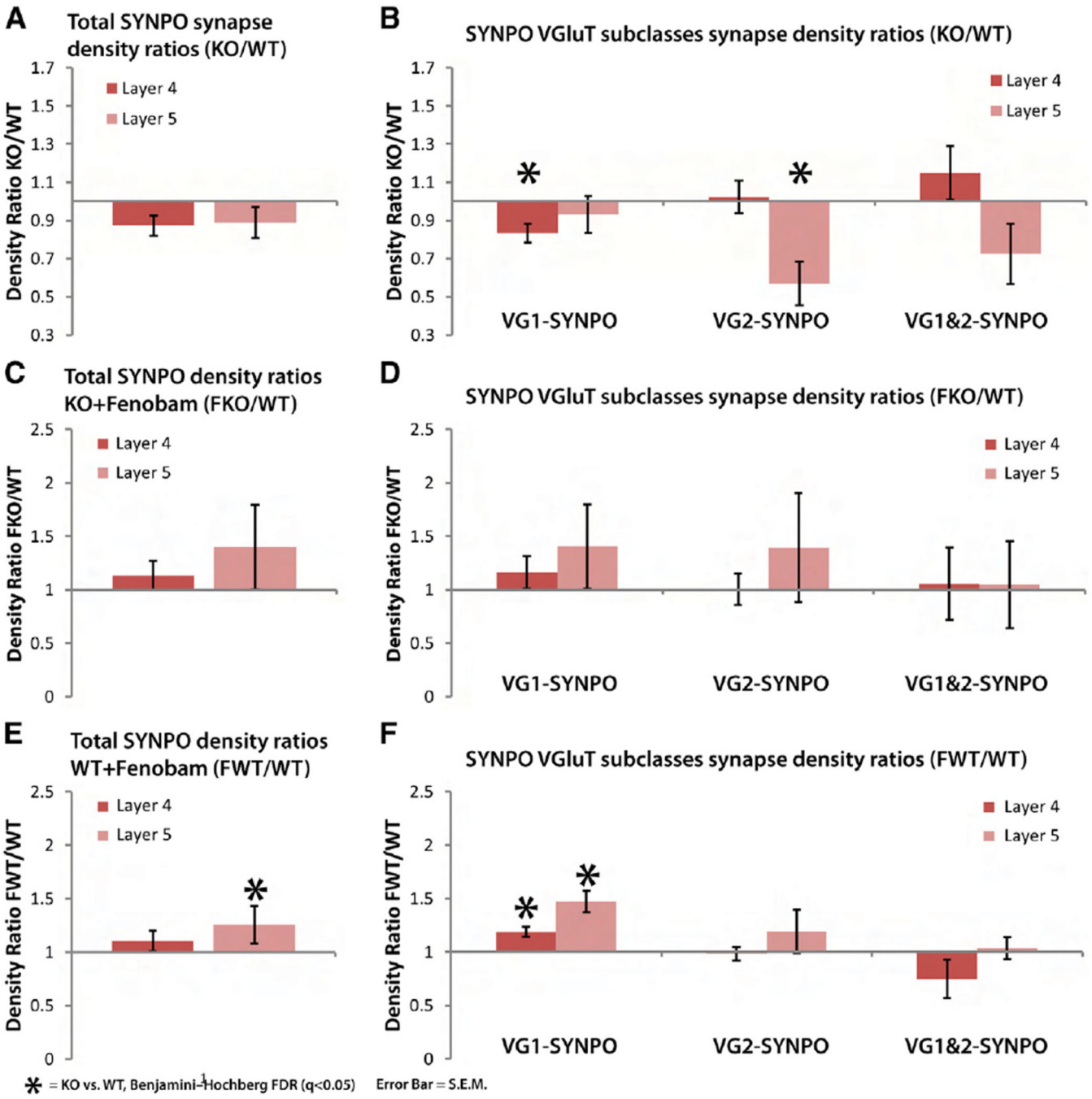

Figure 4. FMRP Loss Induces Fenobam-Reversible Changes in SYNPO Containing Mature Dendritic Spines

(A) Density ratios of KO/WT synapses containing SYNPO, a marker of mature dendritic spines, reveal no significant change in total SYNPO synapse density (n = 6 pairs).

(B) Analysis of specific synaptic classes reveals significant synapse density changes mediated by FMRP loss in layer 4 VGluT1 synapses and layer 5 VGluT2 synapses.

(C and D) Fenobam treatment normalizes to WT SYNPO-containing synapse density across all classes (n = 6 pairs).

(E) Fenobam application in WT animals induces a density increase in layer 5 synapses (n = 5 pairs).
(F) Fenobam-induced SYNPO synapse density increase is specific to VGluT1 class synapses. Error bars, SE. Significance is calculated using paired t tests, and the p values are adjusted via FDR test. $q < 0.05$.

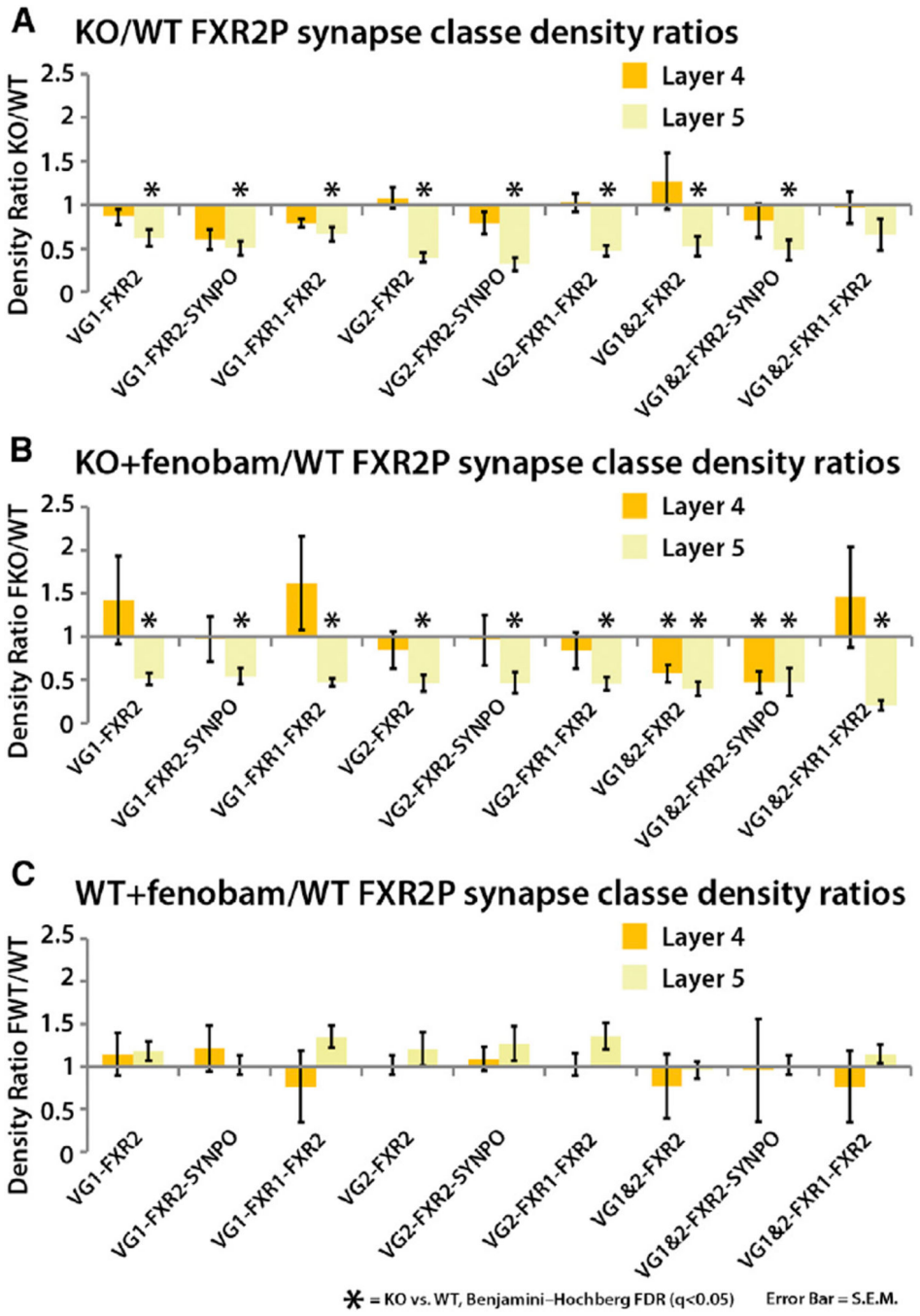

Figure 5. FMRP Loss Specifically Impacts Layer 5 FXR2P-Containing Synapse Density Independent of mGluR5 Signaling

(A) FXR2P-containing synapse density is significantly depressed in layer 5 cortex of *Fmr1* KO in nearly all synapse classes in the study (n = 6 pairs). Layer 4 FXR2P synapses are not perturbed.

(B) This effect is insensitive to fenobam treatment (n = 6 pairs).

(C) Fenobam treatment in WT animals does not affect FXR2P synapses in either layer 4 or 5 (n = 5 pairs). Error bars, SE. Significance is calculated using paired t tests, and the p values are adjusted via FDR test. $q < 0.05$.

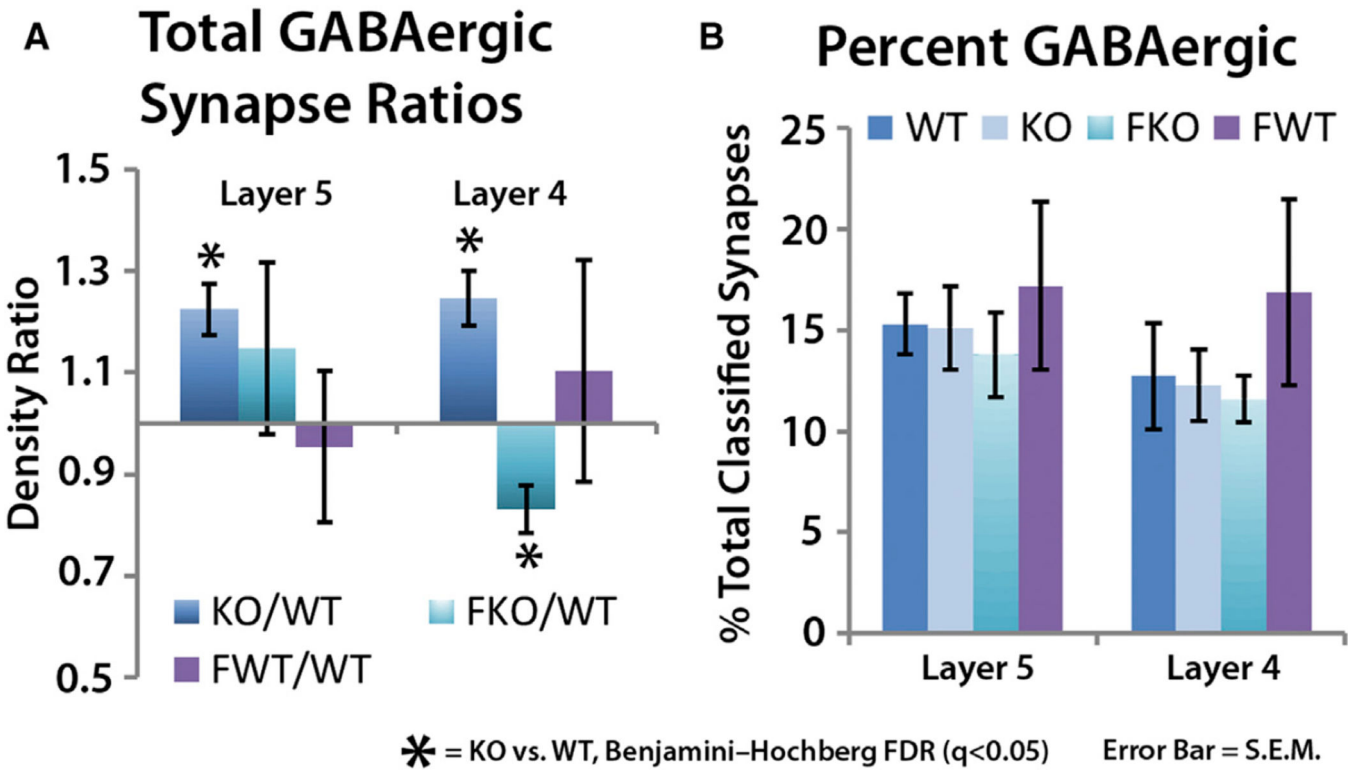

Figure 6. mGluR5-Sensitive Increase in GABAergic Synapse Density in Fmr1 KO

(A) GABAergic synapse density in both layers 5 and 4 are elevated in *Fmr1* KO animals (n = 6 pairs). Fenobam treatment normalizes to WT layer 4 GABAergic synapse density increase, while it reverses layer 5 GABAergic synapse density increase to a significant decrease (n = 6 pairs).

(B) GABAergic synapses as a percent of total classified synapse is not changed. This suggests that GABAergic synapse density is changing in response to glutamatergic synapse density to maintain a specific ratio.

(A and B) Fenobam treatment in WT does not affect total GABAergic synapse density (n = 5 pairs). Error bars, SE. Significance is calculated using paired t tests, and the p values are adjusted via FDR test. $q < 0.05$.

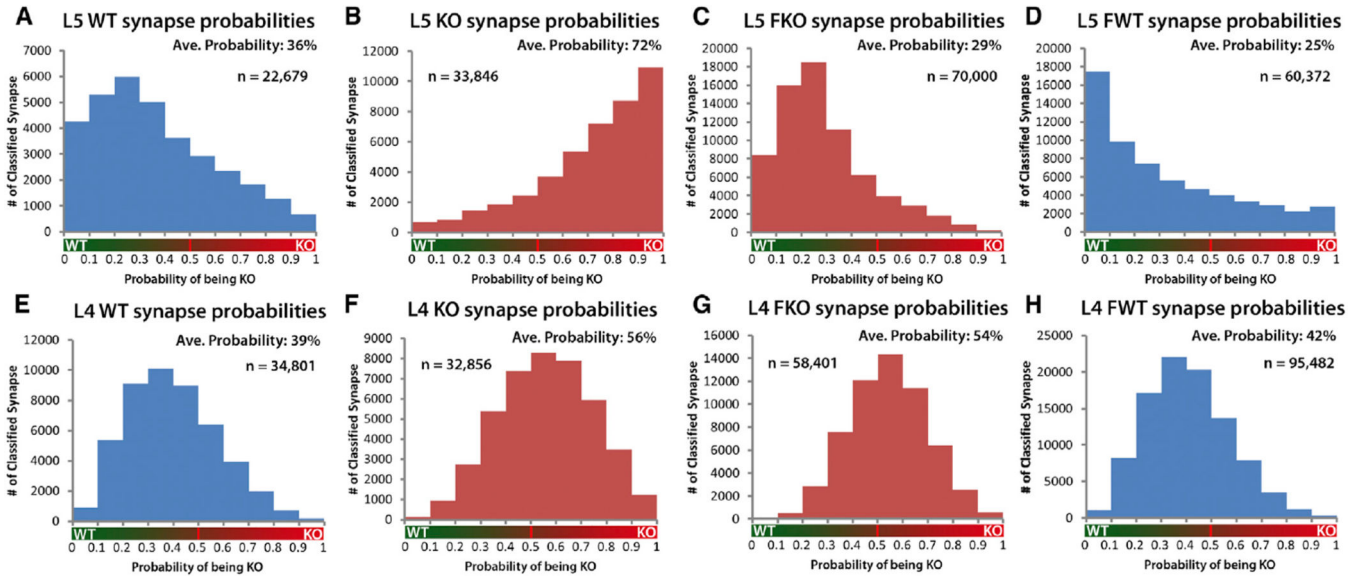

Figure 7. Logistic Regression Analysis of WT, KO, and FKO Synapses Reveals Population Level Shifts in Molecular Features of Synaptic Proteins

(A–H) Population histograms of synapse probabilities of synapses being KO, calculated by regression analysis using synaptic protein feature values for each synapse (KO = 1; WT = 0).

(A and B) Layer 5 population distributions are highly separated. Thus, molecular features of layer 5 KO synapses as a population are clearly distinct from Layer 5 WT synapses.

(A) Layer 5 WT synapse population. (Average probability of being KO = 36%, n = 22,679 synapses, 5 pairs animal.)

(B) Layer 5 KO synapse population. (Average probability of being KO = 72%, n = 33,846 synapses, 5 pairs animal.)

(C) Layer 5 FKO synapse population. Fenobam treatment rescues change in KO synapse molecular features. (Average probability of being KO = 29%, n = 70,000 synapses, 6 pairs animal.)

(D) Layer 5 WT synapse population is not affected by fenobam treatment. (Average probability of being KO = 25%, n = 60,372 synapses, 5 pairs animal.)

(E and F) Layer 4 KO and WT synapse populations, while significantly different, are less so than layer 5 synapse populations.

(E) Layer 4 WT synapse population. (Average probability = 39%, n = 34,801 synapses, 5 pairs animal.)

(F) Layer 4 KO synapse population. (Average probability = 56%, n = 32,856 synapses, 5 pairs animal.)

(G) Layer 4 FKO synapse population. (Average probability = 54%, n = 58,408 synapses, 6 pairs animals.)

(H) Layer 4 WT synapse population is not affected by fenobam treatment. (Average probability of being KO = 42%, n = 95,482 synapses, 5 pairs animal.) Statistical comparison of KO versus WT, FKO versus WT, and KO versus FKO distributions by Kruskal-Wallis are significant ($p < 0.01$).

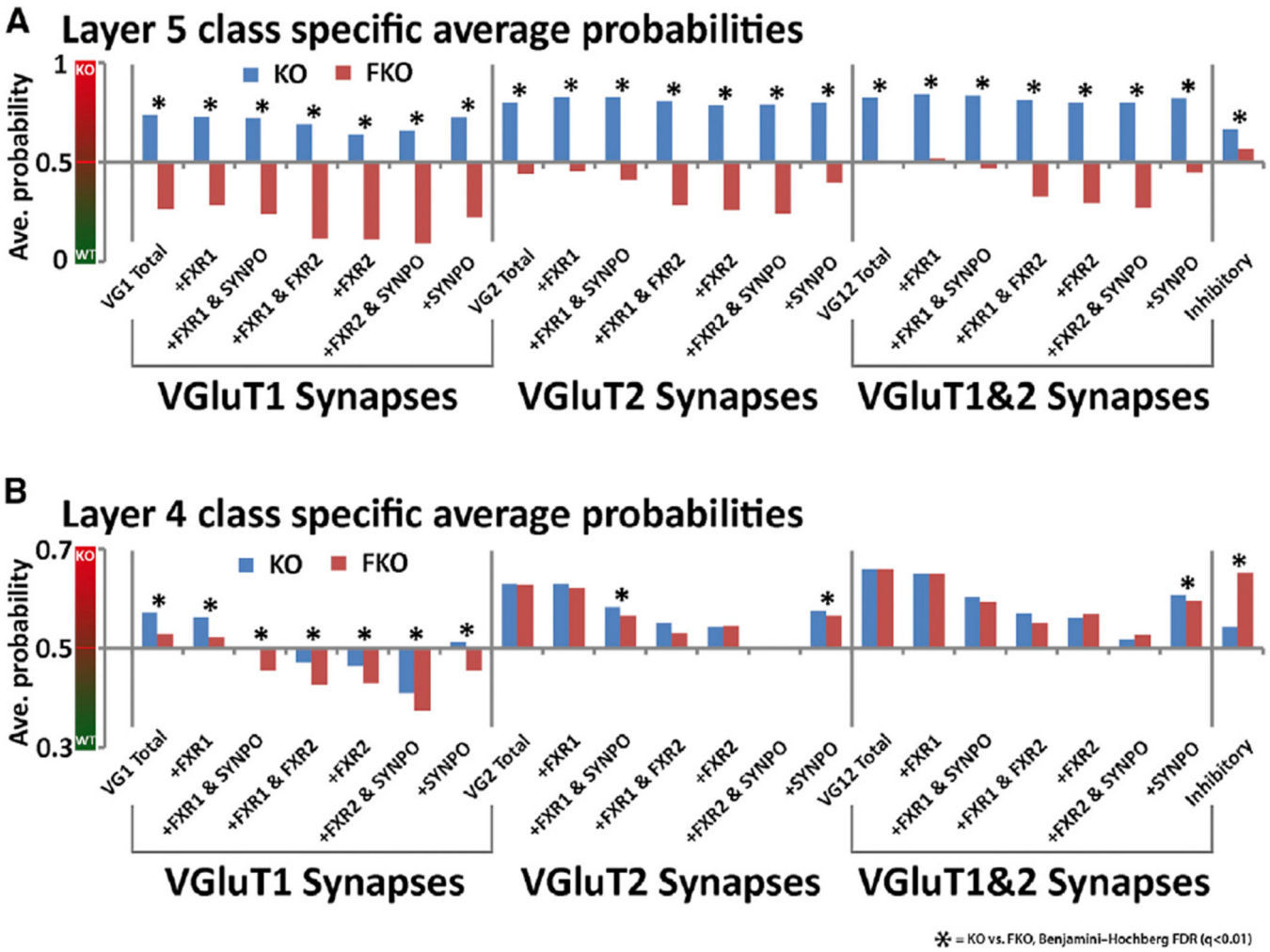

Figure 8. Class-Specific Regression Values Reveal Layer and Class-Specific Efficacy of Fenobam Treatment and Compensatory Effects of FXR2P

(A) Graph of average probability of being a KO for individual synapse classes in layer 5 of the cortex. An average probability that is closer to 1 means the population is closer to KO by molecular features. An average that is closer to 0 means the population is closer to WT by molecular features, and an average at 0.5 means the population is not biased toward WT or KO features. It is clear that in layer 5, all synapse classes, by molecular features, appear KO, and after fenobam treatment all synapses classes appear more WT.

(B) Graph of average probabilities for individual synapse classes in layer 4 of the cortex. Here it is apparent that VGluT2-containing synapses are more KO by molecular features than VGluT1 synapses, and VGluT2-containing synapses are not normalized to WT by fenobam treatment. Also note the more WT average probabilities of FXR2P-containing synapses than synapses that do not. Significance is calculated using Kruskal-Wallis tests, and the p values are adjusted via FDR test. $q < 0.01$.